FeII induced mineralogical transformations of ferric oxyhydroxides into magnetite of variable stoichiometry and morphology

Muhammad Usman, Mustapha Abdelmoula, Khalil Hanna, Brian Grégoire, Pierre Faure, Christian Ruby

Fe^{II} induced mineralogical transformations of ferric oxyhydroxides into magnetite of variable stoichiometry and morphology

M. Usman [a#], M. Abdelmoula [a], K. Hanna [a,c] , B. Grégoire [a], P. Faure [b], C. Ruby [a*]

[a] Laboratoire de Chimie Physique et Microbiologie pour l'Environnement, LCPME, UMR 7564, Institut Jean Barriol, CNRS-Université de Lorraine, 405 rue de Vandoeuvre, 54600, Villers-lès-Nancy, France.

[b] Géologie et Gestion des Ressources Minérales et Energétiques, G2R UMR 7566, CNRS-Université de Lorraine, BP 239, 54506, Vandoeuvre-lès Nancy, France.

[c] Ecole Nationale Supérieure de Chimie de Rennes, UMR CNRS 6226 "Sciences Chimiques de Rennes", Avenue du Général Leclerc, 35708 Rennes Cedex 7, France.

**** Corresponding author:***

LCPME, 405 rue de Vandoeuvre, 54600, Villers-lès-Nancy, France.
Tel: + 33 3 83 68 52 20
Fax: + 33 3 83 27 54 44
Email: christian.ruby@lcpme.cnrs-nancy.fr

[#] Present Address: Institute of Soil and Environmental Sciences, University of Agriculture, Faisalabad, Pakistan

Abstract

The Mössbauer spectroscopy was used to monitor the mineralogical transformations of ferrihydrite (F), lepidocrocite (L) and goethite (G) into magnetite as a function of aging time. Ferric oxyhydroxides were reacted with soluble Fe^{II} and OH^- in stoichiometric amountsto form magnetite at an initial pH of ~ 9.7. Observed transformation extent into magnetite followed the order: F > L > G with almost 30 % of untransformed G after 1 month. The departure from stoichiometry, δ, of magnetite ($Fe_{3-\delta}O_4$) generated from F (δ ~ 0.04) and L (δ ~ 0.05) was relatively low as compared to that in magnetite from G (δ ~ 0.08). The analysis by transmission electron microscopy and BET revealed that generated magnetite was also different in terms of morphology, particle size and surface area depending on the nature of initial ferric oxyhydroxide. This method of preparation is a possible way to form nano-sized magnetite.

***Keywords*:** Ferrihydrite; Lepidocrocite; Goethite; Magnetite; Mössbauer

1. INTRODUCTION

Iron oxyhydroxides are abundant in the environment and influence the biogeochemical cycling and availability of elements. In soils and sediments, iron oxides and oxyhydroxides are commonly found as ferric minerals like goethite, ferrihydrite, hematite and lepidocrocite with different characteristics such as crystallinity, stability, specific surface area and reactivity [1, 2].Due to their high specific surface area, iron oxyhydroxides act as important sorbents for dissolved species. They strongly influence the transport and availability of various nutrients (e.g., C, N, and P) [1, 2] and the mobility of organic and inorganic contaminants [3, 4]. In reduced soil zone, they exist as mixed Fe^{II}-Fe^{III} compounds such as fougerite, the mineral counterpart of the Fe^{II}-Fe^{III} green rust or magnetite ($Fe^{II}Fe^{III}{}_2O_4$) [5, 6]. Due to the presence of structural Fe^{II}, magnetite is considered as reactive and is involved in the reductive transformations of inorganic [7] as well as organic pollutants [3, 8].

Magnetite can be synthesized in laboratory by various biotic and abiotic pathways. Formation of biogenic magnetite was reported as a result of microbial reduction of iron oxyhydroxides [9-12]. Abiotic procedures to form magnetite include partial oxidation of hydroxylated Fe^{II} solution [13] or co-precipitation of Fe^{II} and Fe^{III} salts in aqueous solutions [14]. Magnetite can also be formed by interactions of ferric minerals with aqueous Fe^{II} that induce their structural modifications and bulk phase transformations. These solid state transformations are controlled by various factors like molar ratio $x(Fe^{II}) = Fe^{II}/[Fe^{II} + Fe^{III}]$ [15-18], pH [18, 19], anionic media [20], OH^-/Fe ratio [17, 21] and structure of initial iron oxyhydroxide substrate [22]. The interaction of iron oxides with aqueous Fe^{II} may lead to their transformations into ferric and/or mixed Fe^{II}-Fe^{III} phases. Due to its poor cristallinity, solid state transformations of ferrihydrite are more widely reported. In the presence of low concentration of Fe^{II} species, ferrihydrite was transformed either into goethite [14, 18-20, 23], lepidocrocite [18, 20, 22]or

hematite [18, 24]. At high Fe^{II} amount, mixed Fe^{II}- Fe^{III} minerals such as magnetite [15-18, 22, 25] or green rust [17, 26] were formed from ferrihydrite or lepidocrocite. But, formation of magnetite from goethite by Fe^{II} induced transformations has not been reported yet probably because of its higher thermodynamic stability. Also a comparative quantification of magnetite formation by using stoichiometric conditions from various ferric oxyhydroxides versustime has seldomely been performed. In this study, Mössbauer spectroscopy was used to determine the transformation extent of ferric oxyhydroxides when reacted with hydroxylated Fe^{II} species in stoichiometric quantities to form magnetite. Mössbauer spectroscopy is a potentially useful tool for an accurate quantitative determination of the relative proportions of magnetite and remaining ferric oxyhydroxides. A special attention was devoted to determine the evolution of stoichiometry during transformation by determining Fe^{II} and Fe^{III} contents in magnetite structure where nonstochiometric compound can be written $Fe_{3-\delta}\ O_4$ [7, 27]. Indeed, the reactivity and stability of magnetite is dictated partly by its stoichiometry defined by $x = Fe^{III}/(Fe^{II} + Fe^{III})$ where $0.67 \leq x \leq 1$, with stoichiometric magnetite ($x = 0.67$ or $\delta = 0$) being the most reactive composition [7]. It was shown that stoichiometric magnetite had a lower reduction potential than that of non-stoichiometric magnetite, consistent with higher reactivity toward pollutants such as nitrobenzene compounds [7].

Experiments were conducted on three different iron oxyhydroxides including ferrihydrite, lepidocrocite and goethite. Their transformation extent into magnetite was quantified as a function of aging time (1 hour, 1 day and 1 month). Morphological properties of initial and final products were determined by transmission electron microscopy and multipoint N_2 BET analyses.

2.EXPERIMENTAL SECTION

2.1. Sample preparation

2.1.1. Initial ferric oxyhydroxides substrates

Experiments were conducted with three synthetic iron oxyhydroxides: 2-line ferrihydrite (F), lepidocrocite (γ-FeOOH) (L) and goethite (α-FeOOH) (G). The 2-line ferrihydrite (F) was synthesized according to the method of Schwertmann and Cornell [28]. It was prepared by neutralizing a 0.2 M ferric chloride solution with 1 M NaOH to a pH of around 7.5. The lepidocrocite sample (γ-FeOOH) was synthesized by vigorous air oxidation of the (0.228 M $FeCl_2.4H_2O$ + 0.4 M NaOH) aqueous mixture under a constant neutral pH adjustment [28]. All the Fe^{III} precipitates were washed several times to remove electrolytes, centrifuged and then dried. The goethite (G) sample was prepared by air oxidation of a hydrolyzed $FeSO_4$ solution following a procedure described by Olowe et al. [29].

2.1.2. Transformation experiments

The mineralogical transformations of synthetic ferric oxyhydroxides were examined in batch experiments at room temperature (20 ± 1 °C). To ensure the exclusion of O_2, experiments were conducted in glove box, an anoxic chamber (N_2:H_2 = 98:2). Stoichiometric magnetite ($Fe^{II}\ Fe^{III}_2\ O_4$) contains the Fe^{II}: Fe^{III} ratio of 1:2, so the quantities of ferric oxyhydroxide (Fe^{III}) and Fe^{II} were chosen accordingly. Firstly, a suspension of Fe^{III} oxyhydroxide was prepared (100 mM as Fe^{III} molar concentration) and purged for 1 hour with filter-sterilized N_2 (99.99%) in order to ensure the evacuation of dissolved oxygen which is known to rapidly oxidize Fe^{II} in the presence of oxides at circumneutral pH [30]. The reaction was started by adding $FeSO_4.7H_2O$ with Fe^{II} molar concentration corresponding to 50 mM. An appropriate amount of NaOH (1 M) was then added to the mixture (Fe^{II}/Fe^{III}-oxyhydroxide) to provide the ratio n (OH^-) / n (Fe^{III}) = 1 where n represents the number of moles. Such a quantity of NaOH was required to form stoichiometric magnetite (Reaction 1), thus the starting pH was very

high (~ 9.7). The expected transformation of L and G into magnetite can be achieved through the following reaction:

$$2Fe^{III}OOH + Fe^{II} + 2OH^{-} \Rightarrow Fe^{II}Fe^{III}{}_2O_4 + 2H_2O \quad (1)$$

The suspensions were vigorously stirred for 1 hour, and then aged without stirring at room temperature for 1 hour, 1 day and 1 month.

At specified aging time, the corresponding batch was withdrawn from the series, centrifuged and the solid was dried in glove box for further analysis. To measure the aqueous concentration of Fe^{II} at each time point, aliquots were sampled from the batches, filtered through 0.22 µm filters and added to a tube that contained 2 N HCl. The Fe^{II} concentration in a given solution was determined colorimetrically by the ferrozine assay as previously reported [31]. Total Fe^{II} concentration was measured by performing the ferrozine assay after a full dissolution of the suspension in a concentrated HCl acidic solution. The pH of the suspensions was also measured at each time point.

2.2.Sample characterization

Solid samples were analyzed by Mössbauer spectroscopy. BackscatteringMössbauer spectroscopy using the miniaturized Mössbauer spectrometer MIMOS II [32]was employed to determine the oxidation state of iron and the iron mineralogy of the samples. The filtered samples were inserted into a ~ 3 cm^2 holder specially designed to perform backscatter Mössbauer analyses at room temperature. Reemitted backscattered γ-rays (14.4 keV) were selected by four Si-PIN-diodes detectors. Centre shifts *CS* were reported with respect to that of α-Fe at room temperature. Mössbauer spectra were computer-fitted with either a sum of Lorentzian shape lines or a Voigt profile analyses [33].

Transmission electron microscopy (TEM) observations were carried out with a Philips CM20 TEM (200 kV) coupled with an EDX energy dispersive X-ray spectrometer. The solid powder was re-suspended in 2 mL ethanol under ultrasonication, and a drop of suspension was evaporated on a carbon-coated copper grid which was placed on filter paper.

The specific surface area of synthesized solids was determined by multipoint N_2-BET analysis using a Coulter (SA 3100) surface area analyzer and was found to be 190, 59 and 38 $m^2\ g^{-1}$ for F, L and G respectively.

3. RESULTS AND DISCUSSION

3.1. Initial ferric oxyhydroxides

The Mössbauer spectroscopy was used to characterize ferric oxyhydroxides (F, L and G). Hyperfine parameters corresponding to their spectra recorded at room temperature (Fig. 1) are reported in Table 1. The F and L displayed typical Fe^{III} paramagnetic doublet and G spectrum consisted of a sextet with asymmetrically broadened lines corresponding to a magnetically ordered goethite.

Morphology of initial ferric oxyhydroxides is displayed by TEM images (Fig. S1) where F particles are very small and heavily aggregated. The L crystals are lath-like and elongated with gradually tapering ends like spindles. The length of the crystals is almost homogeneous and varies between 200-300 nm. Crystal needle shapes were identified for G. These crystals vary between 300 and 400 nm in length.

3.2. Transformation products

3.2.1. Mössbauer spectroscopy

Quantification of formed magnetite

The Mössbauer spectra of resulting products obtained by abiotic transformations of initial ferric oxyhydroxides are shown (Fig. 2) along with hyperfine parameters (Table 1). Magnetite formation was quantified after specified aging times of 1 hour, 1 day and 1 month. Stoichiometric magnetite (Fe^{II} Fe^{III}_2 O_4) at room temperature (RT) has a spinel structure whose Mössbauer spectrum at RT is constituted by a superposition of two subspectra associated with the distribution of the iron in the octahedral (B) and tetrahedral (A) sites represented by S_B and S_A respectively. The two valence states on octahedral sites are not distinguishableabove the Verwey transition (125 K)due to a fast electron hopping between Fe^{II} and Fe^{III} in octahedral sites [34, 35]. The different Mössbauer spectra (Fig. 2) are presented here to show the transformation of ferric oxyhydroxides into magnetite at each time point. It was easy to distinguish the appearance of magnetite sextets (S) produced from F and L substrates as both are characterized by doublets (D) in Mössbauer spectra at RT. In contrast, G at the same temperatureis characterized by magnetically ordered component that consist of a sextet with lines that are asymmetrically broadened. The value of G magnetic hyperfine field at room temperature (~ 378 kOe) [34]is much lower than the one obtained for sextets S_A and S_B of magnetite (~ 490 and 460 kOe respectively; see Table 1).

The Mössbauer spectra of the F-M transformations are shown in Fig. 2a. After 1 hour of reaction, a doublet is present in the center of spectrum which reveals the presence of untransformed F, along with magnetic sextets corresponding to a spinel (magnetite). The relative abundance of doublet decreases with the increase in time (Fig. 2a). The magnetic components are very broad and the spectrum is fitted with a distribution of sextets. The broadening of sextets probably corresponds to the crystal growth of a poorly crystallized magnetite. These sextets become more resolved and narrow as the time proceeds from 1 hour

to 1 month that could be linked to the increase in the crystallinity of magnetite. Therefore, only two sextets S_A and S_B are used to fit the spectrum after 1 month. Same trend is observed in case of L (Fig. 2b), except that the transformation extent is lower. The sextets corresponding to magnetite are also more resolved and narrow as compared to magnetite formed from F. No other intermediate minerals are observed during magnetite formation.

The Mössbauer spectra of the G-M transformation exhibit a different trend, in particular in the initial step of the reaction (Fig 2c, G-1 hour). The spectrum is constituted by the sextet S_G of untransformed goethite and two additional components: (i) sextet S_A (H = 491 KOe) and (ii) a Fe^{III} paramagnetic doublet (Δ = 0.71 mms^{-1}). These two last components are attributed to the initial growth of nanocrystalline magnetite, which could be described as the early stages of spinel phase formation on the goethite surface. Indeed, traces of magnetite was also observed by XRD analyses (Fig S2). Small crystal size of magnetite may induce drastic changes in the Mössbauer spectrum (Fig 2c, G-1 hour) which reveals distinct components when compared to the spectrum of the initial goethite (Fig 1). We observe the appearance of a paramagnetic doublet D in the center and a sextet S_A which is superimposed upon those of S_G butwith a magnetic hyperfine field much larger than the one obtained for goethite. The doublet D resembles that of many other paramagnetic Fe^{III} bearing species and is therefore generally not applicable for identification of a spinel phase. However, the concomitant presence of doublet D and sextet S_A similar to that obtained for iron in the tetrahedral site of the spinel inverse structure indicate the presence of nanocrystalline magnetite should not be excluded. This observation could explain consequently the spectral behavior which reveals the collapse of magnetic ordering in octahedral sites governed by a superparamagnetic relaxation [36]. These results could be interpreted by adsorbed Fe^{II} species transforming themselves into growing epitaxial nano-magnetite layer with magnetically short-range ordering. Doublet D could be attributed to Fe^{III} species formed by an electron transfer between adsorbed Fe^{II} species and

Fe^{III} species present on the goethite surface. Such Fe^{II}-Fe^{III} exchange was clearly demonstrated by Williams et al. [37], by using the isotope specificity of ^{57}Fe Mössbauer spectroscopy. Increasing the aging time (1 day to 1 month) enhances the spinel ordering as confirmed by the vanishing of doublet D and the appearance of the classical magnetic components (S_A and S_B). Sextets of magnetite are now clearly resolved and the partial conversion of goethite proceeds by solid-state reaction [17].

All these results consistently show that the F was more reactive to transform into magnetite. Almost 90% of F was transformed into magnetite after aging time of 1h, as compared to 75% of L and 11% of G. After 1 month, almost whole of F and L was transformed (Table 2). Large amount (~ 70%) of G was transformed into magnetite after 1 month, although, goethite is one of the highly stable oxides.The order of reactivity can be classified as F > L > G, which is consistent with previous findings [22]. Pedersen *et al.* reported that the transformation extent decreases by approximately one order of magnitude going from ferrihydrite to lepidocrocite to goethite and the main control on the transformation yield appears to be affiliated with the properties and crystallinity of the iron oxide mineral. This order of reactivity found in present work (F > L > G) is in accordance with surface area, solubility, thermodynamic stability and dissolution data previously reported in literature [22, 23, 38-40]. Size and order of crystal are important determinative factors, affecting dissolution rate of iron oxides as ferrihydrite, an unstable Fe oxide with a large specific surface is more soluble, whereas crystallized iron oxides such as goethite are thermodynamically stable with a relatively low dissolution rate [22, 23, 40].

Stoichiometry of final magnetite

The degree of stoichiometry (δ) of magnetite $Fe_{3-\delta}O_4$ was quantitatively determined by using the Mössbauer data obtained during transformations (Table 1). The stoichiometry is defined by $x = Fe^{III}/(Fe^{II} + Fe^{III})$ where $0.67 \leq x \leq 1$ with stoichiometric magnetite corresponding to $x = 0.67$ and $\delta = 0$. Stoichiometry of magnetite was calculated as a function of aging time from experimental values of relative areal (RA) of both sextets, S_A and S_B, as explained by Zegeye *et al.*[9]. Because Mössbauer spectroscopy was not always able to detect unambiguously the presence of low amount of hematite (< 10 wt%) in the presence of magnetite [41], XRD was used to confirm the absence of αFe_2O_3 in the final products (Figure S2). A slight departure from stoichiometry was observed for final magnetite obtained from F ($\delta \sim 0.04$) and L ($\delta \sim 0.05$) after 1 month. Magnetite formed from G was the least stoichiometric as the transformation was not fully accomplished. A higher departure ($\delta \sim 0.2$) was observed for G product after 1 day that evolved towards lower value ($\delta \sim 0.08$) in 1 month. On the contrary to magnetite formed from G, slight increase in departure from stoichiometry of magnetite ($\delta = 0.005$-0.05) in L product was observed with an increase in aging time. Stoichiometric magnetite ($\delta = 0$) was not obtained in any of the final product regardless of initial ferric oxyhydroxide, although, the stoichiometric conditions were imposed in the initial suspension. It suggests that small part of the initial soluble Fe^{II} did not incorporate in the final solid product leading to a non-stoichiometric magnetite. Similarly it was reported elsewhere that excessive washing of stoichiometric magnetite caused the magnetite to become oxidized due to Fe^{II} dissolution [7, 8]. On the other hand, biogenic magnetite was stoichiometric with $\delta \sim 0$ when the mineralogical transformation of L was investigated in a *Shewanella putrefaciens* culture under anaerobic conditions using methanoate as the electron source for almost 1 month [9]. Thus, stoichiometry of final magnetite could vary according to the nature of initial ferric oxyhydroxide, aging time and the pathway of magnetite formation. Stoichiometric magnetite may form directly by

coprecipitation [14] or bioreduction of lepidocrocite [9], while topotactic formation from ferric oxyhydroxide leads to non-stoichiometric phases.Stoichiometry of magnetite is an important characteristic as it can influence its reactivity.

3.2.2. Evolution of pH and concentration of soluble Fe^{II}

Total and soluble Fe^{II} concentration, pH in the oxide suspensions at specified aging times during transformation process are reported in Table 2. The pH at the start of reaction was almost same for F, L and G (~ 9.7). This value is significantly higher than the pH of precipitation (~ 7) of $Fe(OH)_2$ corresponding to the initial Fe^{II} concentration. As the reaction proceeded, a decrease in pH was observed as the OH^- species were consumed to form magnetite as shown in reaction (1). Decrease in pH could positively be correlated to the dissolution of the initial $Fe(OH)_2$ precipitates into hydroxylated Fe^{II} species adsorbed on the ferric oxyhydroxides. After 1 month, the pH observed for F and L suspension was ~ 5.5 while pH was higher (~ 7.5) for partially transformed G. The total Fe^{II} concentration of the final suspension (transformation product and solution) was measured during experiment and it was almost the same as the initial concentration (50 mM) suggesting the absence of Fe^{II} oxidation (Table 2). On the other hand, concentration of soluble iron was very low after 1 hour of aging time. Almost 98% of the input Fe^{II} amount was rapidly removed from the aqueous solution although the extent of transformation of F, L and G was different. It is probably due to sorption of Fe^{II} species on iron oxide surface as reported elsewhere [25, 38]. In this case, Fe^{II}-to-Fe^{III} electron transfer and precipitation processes are contributing to the observed sorption phenomena. These observations are consistent with literature [40] stating that the Fe^{II} adsorption edge was the same for the three oxyhydroxide phases: goethite, hematite and ferrihydrite. At pH > 7.5, the adsorption of Fe^{II} onto iron oxyhydroxide phases reach 100 %

277 regardless of the tested oxide. Calculations using PHREEQC2 [42] of the pH dependence of
278 adsorption of Fe^{II}on F, L or G confirms that all $Fe^{II}$is adsorbed at a pH higher than 7. A
279 progressive release of Fe^{II} in solution (~ 5-8 mM) was observed during the formation of
280 magnetite from F and L when the pH reached a value lower than 7 (Table 2). This
281 phenomenon could be attributed to a progressive desorption of previously sorbed Fe^{II} species.
282 After 1 month of aging time, the transformation extent of F and L was very close to 100%
283 (Table 1). The departure from stoichiometry of the obtained magnetite is $\delta \sim 0.04$, its chemical
284 composition is therefore $Fe^{III}_{2.08}Fe^{II}_{0.88}O_4$ (Fe^{II} : Fe^{III} of 2.36 instead of 2 for $\delta \sim 0$). By
285 considering that all the initial Fe^{III} species (100 mM) were present inside the magnetite, 42.4
286 mM of Fe^{II} are taking part in the formation reaction. Therefore, a concentration of 7.6 mM of
287 unreacted Fe^{II} species is expected, which is in good agreement with that measured in solution
288 after 1 month of reaction for F and L (Table 2). On the other hand, pH was still higher than 7
289 after one month of G transformation therefore soluble Fe^{II} was almost negligible.

290

291 **3.2.3. Morphological properties of transformation products**

292 The morphology of the particles produced is available to clarify the transformation of ferric
293 oxyhydroxides into magnetite as shown by transformation products after 1 month (Fig. 3).
294 TEM findings were consistent with Mössbauer results. Variations in size and shape of
295 magnetite particles were observed among the products of tested ferric oxyhydroxides.
296 Magnetite particles resulting from F transformation (Fig. 3, F-1 month) were smaller with
297 non-uniform size or shape. The shape of magnetite particles was between hexagonal to
298 octahedral in the transformation products of both G and L substrates (Fig. 3, G-1month, L-
299 1month). TEM images showed that there was still large amount of G which was not
300 transformed into magnetite, while traces of L were also visible. A difference in morphology

and particle size of generated magnetite was observed dependent on the nature of initial substrates. Indeed, the transformation of ferrihydrite produced small magnetite particles (< 50 nm) while those found in the transformation products of L or G have larger particles (magnetite particles with 70-80 nm and 200-300 nm in L and G products respectively). It seems that magnetite, formed by reaction with Fe^{II}, has morphology and particle size similar to those of the initial oxyhydroxides which occurs in topotactic conversion of initial compounds to magnetite [14, 43]. In addition, the Mössbauer spectra of magnetite formed from ferrihydrite displays broad lines, often caused by a structural disorder. This observation is also in favor of a topotactic formation of magnetite onto poorly crystallized ferrihydrite. In contrast, well ordered magnetite with sharp Mössbauer lines was obtained from crystallized iron oxides (i.e. L and G) (Fig. 2&3).

Since final product of G transformation is a mixture of goethite and magnetite, only magnetite produced from F and L were characterized by N_2 adsorption isotherm. The specific surface area (SSA) experimental value of magnetite, formed from F or L, determined by the BET method was found to be 40 ± 2 and 20 ± 2 m^2 g^{-1}, respectively. The radius of the supposed spherical particles (the density of magnetite, $\rho = 5.15 \times 10^6$ g/m^3) can be related to the surface area as $A = 6/ (\rho.d)$. Thus, the calculated average diameter of a supposed spherical particle is ~ 30 nm and ~ 60 nm for magnetite from F for L respectively, which is consistent with the average size estimated by the TEM observations. The size of magnetite particles in F product falls in the size range of nano-particles of magnetite observed for commercially available nano-magnetite (i.e. 48 m^2 g-1, 30 nm) [44].

5. CONCLUSION

The transformation of ferric oxyhydroxides into magnetite was investigated in the present work which contributes to our understanding of the magnetite formation in natural environments. Order of reactivity to transform into magnetite was F > L > G. The evolution of stoichiometry of final magnetite was also monitored. This study demonstrates that the transformation of ferric oxyhydroxides in the presence of Fe^{II}can be affected by many factors including mineralogy of initial oxyhydroxide, aging time and solution chemistry. Magnetite was the product, with variable stoichiometry, particle size and surface area, obtained from different ferric oxyhydroxides. Magnetite was non-stoichiometric regardless of the initial ferric oxyhydroxide although stoichiometric conditions were imposed. In the case of goethite, it is more striking as observed by Mössbauer spectroscopy over aging time. The results suggest a solid-state transformation of goethite into magnetite with an electron transfer driving the spinel ordering between adsorbed Fe^{II} and the ferric oxide. Moreover, reactivity of the magnetite could be different depending on its source of ferric mineral which need to be explored for remediation purposes. For example, magnetite produced from ferrihydrite was more close to stoichiometry with smaller particles and higher surface area; all these factors could possibly contribute towards its high reactivity. Fe^{II}-induced transformations of ferric oxyhydroxides could be a novel way to synthesize nano-sized particles of magnetite. These findings have important implications for remediation technologies using magnetite as catalyst, and also for the natural attenuation of contaminants in soils and sediments.

Acknowledgements

The authors acknoweledge the financial support of Higher Education Commission of Pakistan (HEC), Agence Nationale de la Recherche (ANR) and Agence de l'Environnement et de la Maitrise de l'Energie (ADEME) (Programme ECOTECH 2009, Production durable de Technologies de l'Environnement, CERVEAU NP, décision attributive d'aide n°

348 0994C0103). We are also thankful to J. Ghanbaja for TEM analyses. We would like to thank
349 the Région Lorraine and the GISFI (Groupement d'Intérêt Scientifique sur les Friches
350 Industrielles) for financial support.
351

References

[1] W. Stumm, B. Sulzberger, Geochim. Cosmochim. Acta, 56 (1992) 3233-3257.

[2] R.M. Cornell, U. Schwertmann, The Iron Oxides: Structure, Properties, Reactions, Occurrence and Uses, Wiley-VCH, 1996.

[3] M. Elsner, R.P. Schwarzenbach, S.B. Haderlein, Environ. Sci. Technol. 38 (2003) 799-807.

[4] K. Hanna, B. Rusch, L. Lassabatere, A. Hofmann, B. Humbert, Geochim. Cosmochim. Acta, 74 (2010) 3351-3366.

[5] M. Abdelmoula, F. Trolard, G. Bourrié, J.M.R. Génin, Hyperfine Interact. 112 (1998) 235-238.

[6] F. Trolard, J.M.R. Génin, M. Abdelmoula, G. Bourrié, B. Humbert, A. Herbillon, Geochim. Cosmochim. Acta, 61 (1997) 1107-1111.

[7] C.A. Gorski, M.M. Scherer, Am. Mineral. 95 (2010) 1017-1026.

[8] C.A. Gorski, M.M. Scherer, Environ. Sci. Technol. 43 (2009) 3675-3680.

[9] A. Zegeye, M. Abdelmoula, M. Usman, K. Hanna, C. Ruby, Am. Mineral. 96 (2011) 1410-1413.

[10] E.J. Oloughlin, C.A. Gorski, M.M. Scherer, M.I. Boyanov, K.M. Kemner, Environ. Sci. Technol. 44 (2010) 4570-4576.

[11] J.M. Zachara, R.K. Kukkadapu, J.K. Fredrickson, Y.A. Gorby, S.C. Smith, Geomicrobiol. J. 19 (2002) 179-207.

[12] R.S. Cutting, V.S. Coker, J.W. Fellowes, J.R. Lloyd, D.J. Vaughan, Geochim. Cosmochim. Acta, 73 (2009) 4004-4022.

[13] J.M.R. Génin, C. Ruby, A. Géhin, P. Refait, C. R. Geosci. 338 (2006) 433-446.

[14] E. Tronc, P. Belleville, J.P. Jolivet, J. Livage, Langmuir, 8 (1992) 313-319.

377 [15] C.M. Hansel, S.G. Benner, S. Fendorf, Sci. Technol. 39 (2005) 7147-7153.
378 [16] Y. Tamaura, K. Ito, T. Katsura, J. Chem. Soc. Dalton. (1983) 189-194.
379 [17] C. Ruby, A. Géhin, M. Abdelmoula, J.-M.R. Génin, J.-P. Jolivet, Solid State Sci. 5
380 (2003) 1055-1062.
381 [18] H. Liu, M. Ma, M. Qin, L. Yang, Y. Wei, J. Solid State Chem. 183 (2010) 2045-2050.
382 [19] B.-H. Jeon, B.A. Dempsey, W.D. Burgos, Environ. Sci. Technol. 37 (2003) 3309-3315.
383 [20] H. Liu, H. Guo, P. Li, Y. Wei, J. Solid State Chem. 181 (2008) 2666-2671.
384 [21] T. Ishikawa, Y. Kondo, A. Yasukawa, K. Kandori, Corros. Sci. 40 (1998) 1239-1251.
385 [22] H.D. Pedersen, D. Postma, R. Jakobsen, O. Larsen, Geochim. Cosmochim. Acta, 69
386 (2005) 3967-3977.
387 [23] N. Yee, S. Shaw, L.G. Benning, T.H. Nguyen, Am. Mineral. 91 (2006) 92-96.
388 [24] H. Liu, P. Li, B. Lu, Y. Wei, Y. Sun, J. Solid State Chem. 182 (2009) 1767-1771.
389 [25] J.P. Jolivet, P. Belleville, E. Tronc, J. Livage, Clay. Clay Miner. 40 (1992) 531-539.
390 [26] M. Usman, K. Hanna, M. Abdelmoula, A. Zegeye, P. Faure, C. Ruby, Appl. Clay Sci. In
391 Press (2011) DOI:10.1016/j.clay.2011.10.008.
392 [27] F.C. Voogt, T. Fujii, P.J.M. Smulders, L. Niesen, M.A. James, T. Hibma, Phys. Rev. B,
393 60 (1999) 11193-11206.
394 [28] U. Schwertmann, R.M. Cornell, Iron Oxides in the Laboratory: Preparation and
395 Characterization, Wiley-VCH, New York, 2000.
396 [29] A. Olowe, P. Refait, J. Génin, Hyperfine Interact. 57 (1990) 2037-2043.
397 [30] H. Tamura, S. Kawamura, M. Hagayama, Corros. Sci. 20 (1980) 963-971.
398 [31] E. Viollier, P.W. Inglett, K. Hunter, A.N. Roychoudhury, P. Van Cappellen, Appl.
399 Geochem. 15 (2000) 785-790.
400 [32] G. Klingelhöfer, B. Fegley Jr, R.V. Morris, E. Kankeleit, P. Held, E. Evlanov, O.
401 Priloutskii, Planet. Space Sci. 44 (1996) 1277-1288.

[33] D.G. Rancourt, J.Y. Ping, Nucl. Instrum. Meth. B, 58 (1991) 85-97.

[34] E. Murad, J.H. Johnston, Mössbauer Spectroscopy Applied to Inorganic Chemistry, Plenum, New York, 1984.

[35] R.E.Vandenberghe, C.A. Barrero, G.M. Da Costa, E.Van San, E. De Grave, Hyperfine Interact. 126 (2000) 247-259.

[36]A. Hartridge, A. K. Bhattacharya, M. Sengupta, C. K. Majumdar, D. Das, S. N. Chintalapudi, J. Magn. Magn. Mater. 176 (1997) L89-L92.

[37] A.G.B. Williams, M.M. Scherer, Environ. Sci. Technol. 38 (2004) 4782-4790.

[38] B. Lu, H. Guo, P. Li, H. Liu, Y. Wei, D. Hou, J. Solid State Chem. 184 (2011) 2139-2144.

[39] U. Schwertmann, Plant Soil, 130 (1991) 1-25.

[40] E. Liger, L. Charlet, P. Van Cappellen, Geochim. Cosmochim. Acta, 63 (1999) 2939-2955.

[41] M. Gotić, G. Goščec, S. Musić, J. Mol. Struct. 924 (2009) 347.

[42] D.L. Parkhurst, C.A.J. Appelo, U.S. Geo. Surv. Water-Resour. Invest. Rep. 1999, 99-4259.

[43] J.K. Fredrickson, J.M. Zachara, D.W. Kennedy, H. Dong, T.C. Onstott, N.W. Hinman, S.-m. Li, Geochim. Cosmochim. Acta, 62 (1998) 3239-3257.

[44] X. Zeng, K. Hanna, A.T. Lemley, J. Mol. Catal. A: Chem. 339 (2011) 1-7.

Figure captions

Figure 1: Mössbauer spectra of original ferric oxyhydroxides, ferrihydrite (F), goethite (G) and lepidocrocite (L). Hyperfine parameters corresponding to these spectra are presented in Table 1.

Figure 2: Mössbauer spectra of the transformation products of (a) F-ferrihydrite, (b) L-lepidocrocite and (c) G-goethite, obtained after aging time of 1 hour, 1 day and 1 month. Hyperfine parameters corresponding to these spectra are presented in Table 1. The percentage corresponds to the relative emission of the most intense lines.

Figure 3: Bright field TEM images showing the transformations products after an aging time of 1 month where M stands for magnetite, L for lepidocrocite and G for Goethite.

437 # Tables

Table 1:Mössbauer hyperfine parameters of the spectra presented in Figure 1 and Figure 3. *CS:* centre shift with respect to metallic α-Fe at room temperature; *Δ*: quadrupole splitting in the paramagnetic state or *ε*: quadrupole shift; *H:* Hyperfine magnetic field; *RA:* relative area and δ: departure from stoichiometry of non-stoichiometric magnetite ($Fe_{3-\delta}O_4$) determined by classical Mössbauer analysis (δ = 0 for stoichiometric magnetite, Fe_3O_4).

* δ calculation is possible only when fitting of magnetite spectrum is done with two sextets; S_A and S_B.

Sample	**Component**	***CS*** **(mm s^{-1})**	***Δ or ε*** **(mm s^{-1})**	***H*** **(kOe)**	***RA*** **(%)**	**Stoichiometry δ**
Ferrihydrite	D	0.35	0.68	-	100	-
F-1 hour	D	0.38	0.71	-	9	
	S1	0.30	0.20	459	13	
	S2	0.42	-0.07	430	68	*
	S3	0.25	0.01	485	10	
F-1 day	D	0.34	0.61	-	4	
	S1	-0.01	0.005	476	12	*
	S2	0.346	0.02	407	59	
	S3	0.678	0.02	462	25	
F-1 month	D	0.30	0.77	-	2	
	S_A	0.27	0	479	40	**δ = 0.04**
	S_B	0.64	0	444	58	
Goethite	S_G	0.38	-0.13	351	100	-
G-1 hour	D	0.39	0.72	-	7	
	S_G	0.37	-0.13	364	89	*
	S_A	0.37	0	491	4	
G-1 day	S_G	0.38	-0.13	378	68	
	S_B	0.64	-0.02	460	7	**δ = 0.23**
	S_A	0.32	-0.004	491	25	
G-1 month	S_A	0.31	0.008	491	32	
	S_B	0.66	-0.003	458	35	**δ = 0.08**
	S_G	0.38	-0.14	377	33	
Lepidocrocite	D	0.48	0.54	-	100	-
L-1 hour	D	0.39	0.56	-	26	
	S_A	0.32	0.01	484	25	**δ = 0.005**
	S_B	0.61	-0.05	452	49	
L-1 day	D	0.39	0.56	-	2	
	S_A	0.33	0.006	488	47	**δ = 0.045**
	S_B	0.63	0	453	51	
L-1 month	D	0.40	0.53	-	2	
	S_A	0.33	0.01	490	41	**δ = 0.05**
	S_B	0.58	-0.02	456	57	

438

Table 2: Percentage of magnetite formation measured by Mössbauer spectroscopy and variousconcentrations measured in the supernatant.

Sample	Magnetite formation (%)	pH	Total Fe^{II} concentration [mM]	Soluble Fe^{II} concentration [mM]
Ferrihydrite				
F- t = 0*	-	9.7	-	
F-1 hour	91	6.9	49	Not detected
F-1 day	96	6	48	2
F-1 month	98	5.6	49	8
Goethite				
G- t = 0*	-	9.8	-	
G-1 hour	11	8.4	47	Not detected
G-1 day	32	8.2	48	Not detected
G-1 month	67	7.5	49	Not detected
Lepidocrocite				
L- t = 0*	-	9.6	-	
L-1 hour	74	7.8	49	Not detected
L-1 day	98	6.4	48	2
L-1 month	98	5.6	47	5.5

* The pH was measured just after the addition of NaOH into the Fe^{III}-Fe^{II} suspension

457 **Figure 1:**

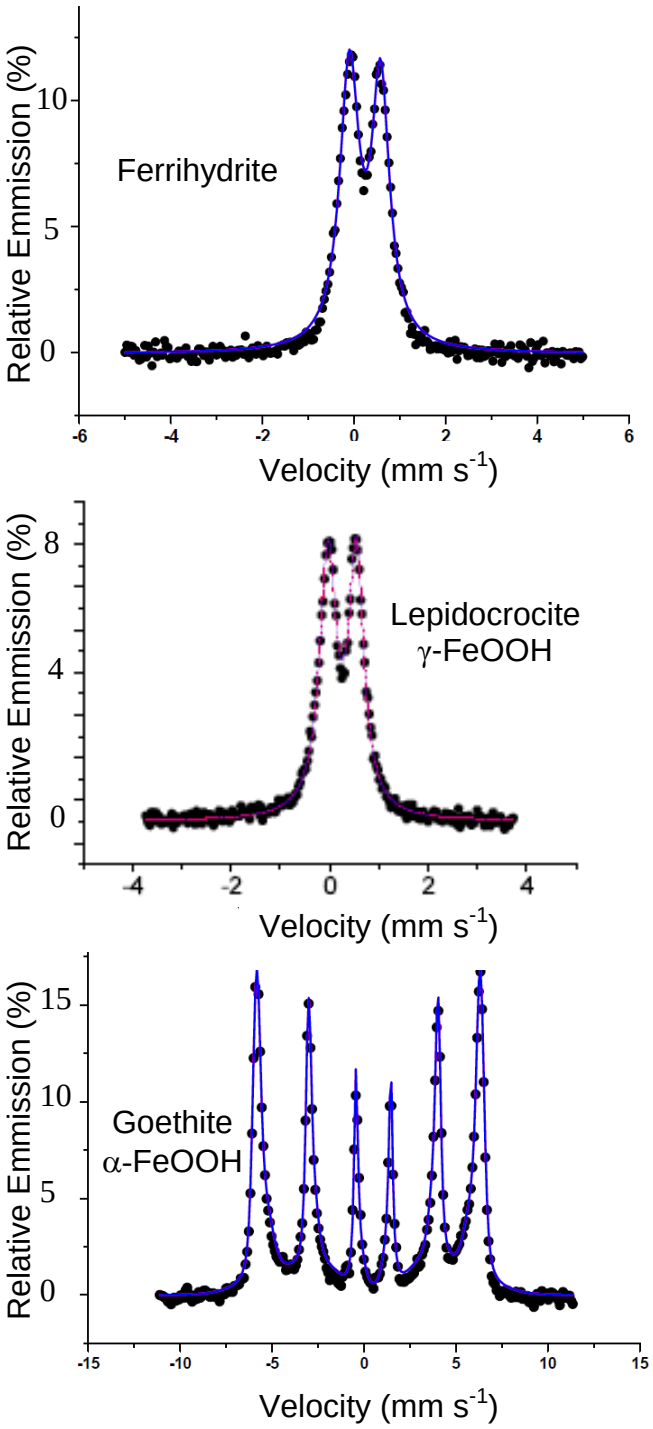
Relative Emmission (%)
Ferrihydrite
Velocity (mm s-1)
Relative Emmission (%)
Lepidocrocite
γ-FeOOH
Velocity (mm s-1)
Relative Emmission (%)
Goethite
α-FeOOH
Velocity (mm s-1)

Figure 2:

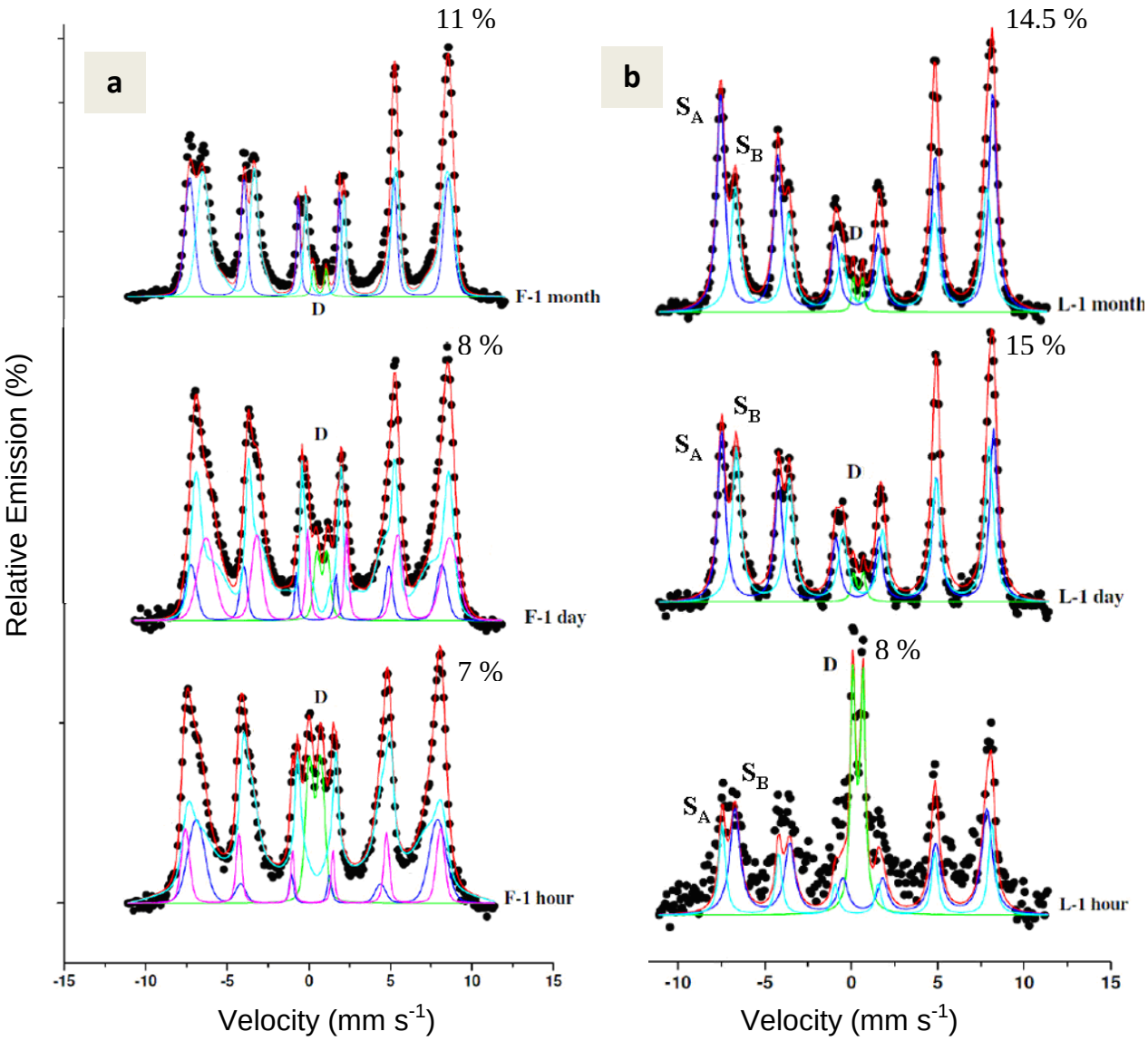
a
b
11 %
14.5 %
8 %
15 %
7 %
8 %
D
S_A
S_B
F-1 month
F-1 day
F-1 hour
L-1 month
L-1 day
L-1 hour
Relative Emission (%)
Velocity (mm s^{-1})
-15
-10
-5
0
5
10
15

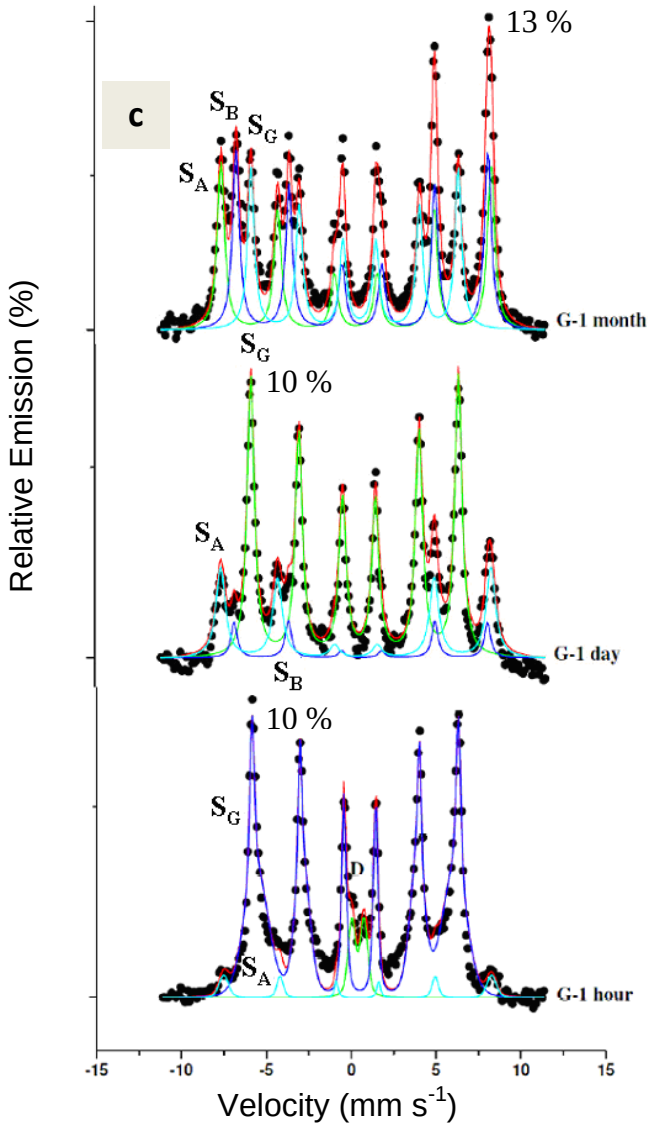
c
13 %
S_B
S_G
S_A
G-1 month
S_G
10 %
S_A
G-1 day
S_B
10 %
S_G
D
S_A
G-1 hour
Relative Emission (%)
-15
-10
-5
0
5
10
15
Velocity (mm s-1)

Figure 3:

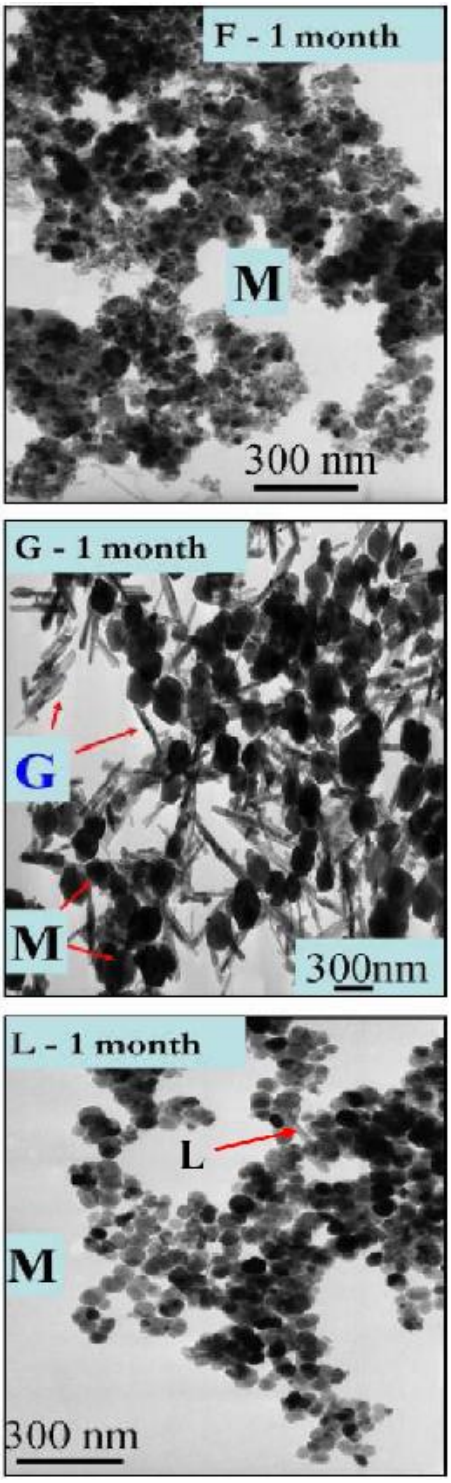

458

Supporting information of Manuscript JSSC-12-104

Figure S1: Bright field TEM images showing initial ferric oxyhydroxides (F-ferrihydrite, L-lepidocrocite and G-goethite).

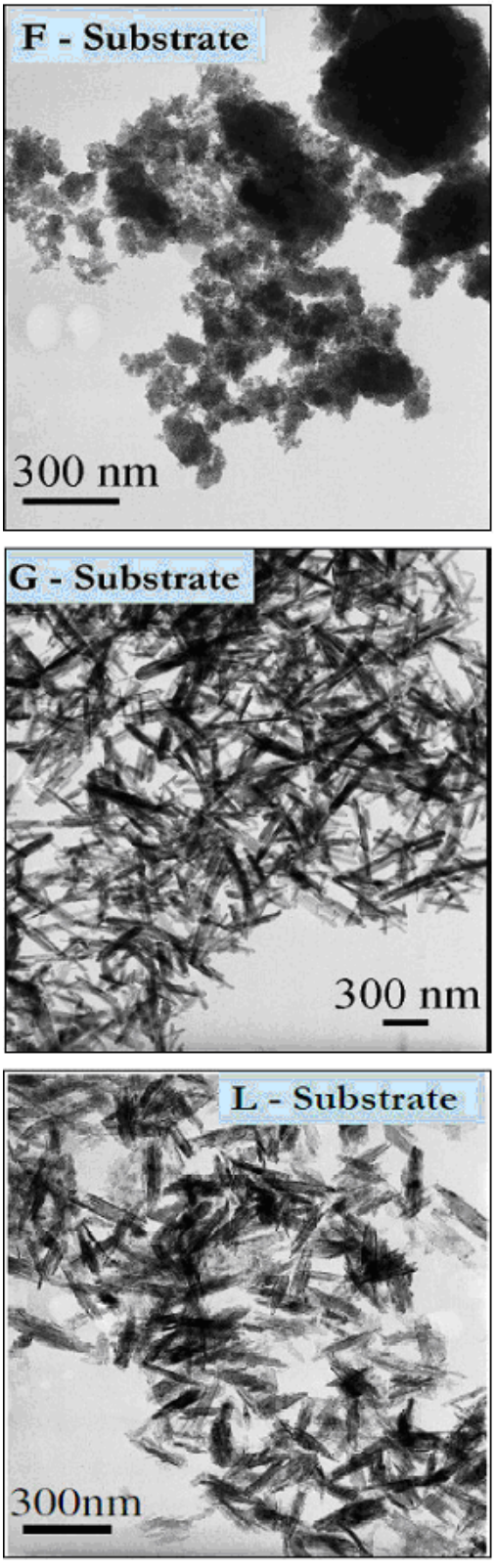

Figure S2:Evolution of the X-ray diffraction patterns of the various samples as a function of aging time. Initial substrate is Ferrihydrite F (a), Lépidocrocite L (b) and Goethite G (c). M stands for magnetite

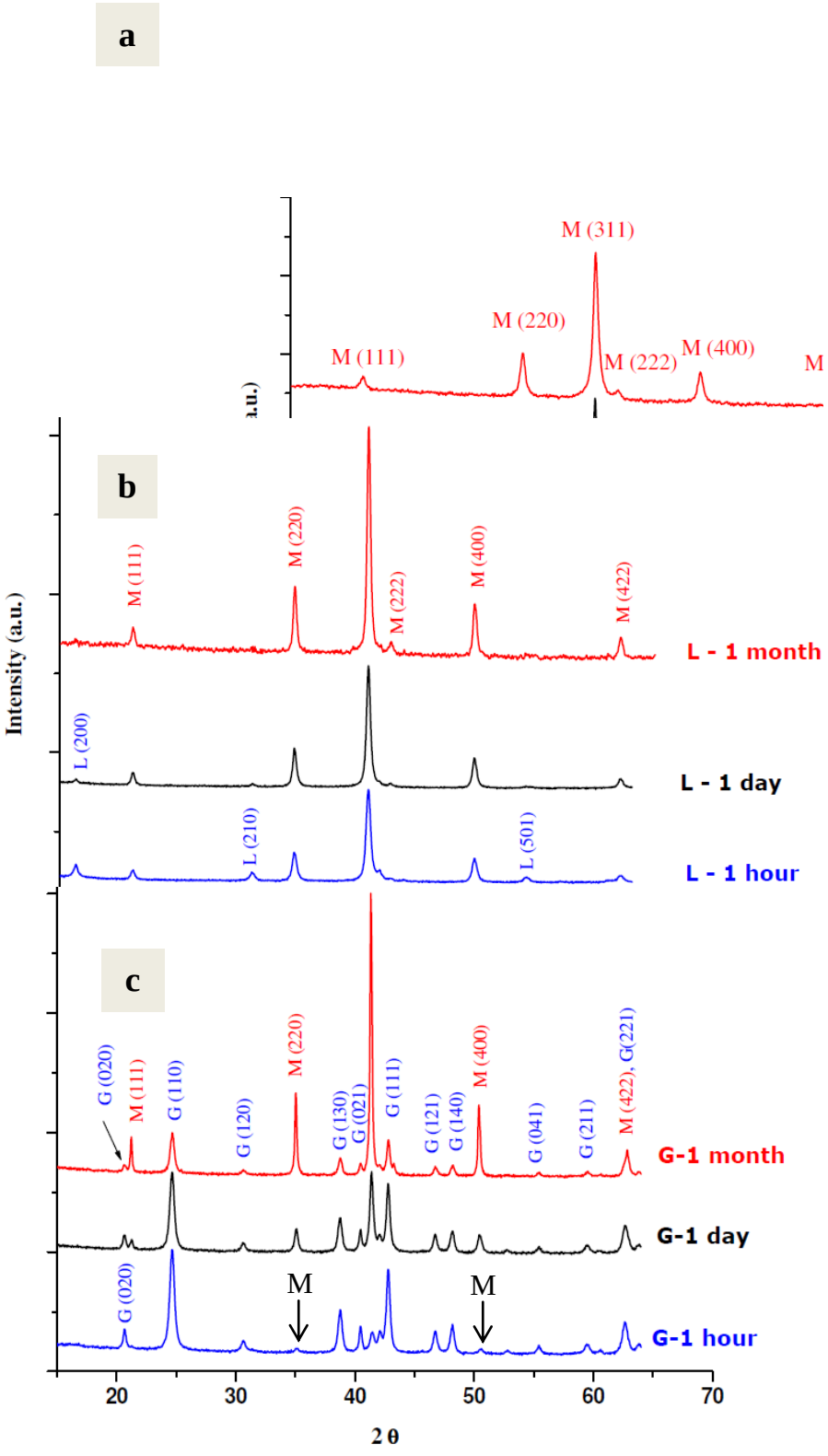

516